Network Capacity Optimisation, Part I: Cellular Radio Networks

Jörg Habetha
Philips Research, Weisshausstrasse 2, D-52066 Aachen, Germany

Jens Wiegert
Aachen University of Technology, Chair of Communication Networks, Kopernikusstr. 16, D-52074 Aachen, Germany

Abstract — **In this paper an analytical approach to calculate the average data throughput of a cellular radio communication system is presented. For this purpose the spatial distribution of the *Carrier to Interference Ratio* (C/I) inside a radio cell is derived. The C/I determines the average data rate that can be achieved at a specific position and finally on average in the overall system.**

At first, analytical formula are derived for a cellular system with no power control and no adaptive modulation or coding. In a next step it is shown how these formula change in the presence of adaptive modulation/coding and power control.

Adaptive Modulation/coding is an important feature of most of the third generation wireless communication systems like GPRS, UMTS, HIPERLAN/2 and IEEE 802.11a. In this paper the analytical approach is applied to HIPERLAN/2 and is to used optimise network capacity and to derive regions of a radio cell, in which a certain combination of modulation and coding scheme can be applied.

I. Introduction

In analytical considerations, radio cells are traditionally represented as hexagons (cf. Fig. 1).

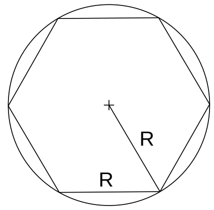

Fig. 1: Hexagonal Cell Representation

Cells are grouped into clusters, in which every frequency channel is used only once. The size and number of cells per cluster determines the re-use distance of a frequency channel [1, 2]. Fig. 2 illustrates the cell structure for the case of a cluster-size of 7. In this Figure as well as in the following omnidirectional and un-sectored antennas are assumed.

It can be depicted from Fig. 2 that in the considered example a cell receives interference from six surrounding cells that are at the same distance from the center cell and separated from each other by an angular distance of 60 degrees. We are neglecting the interference from cells that are more than one reuse distance away from the considered cell, which is a realistic assumption, especially at high frequencies. Due to the chosen hexagonal cell modelling, the number of cells in re-use distance using the same frequency(ies) is always equal to 6 and their angular distance is always 60 degrees. At different cluster sizes only the distance of the interfering cells changes. In any case this distance D is proportinal to the cluster size n and the cell radius R:

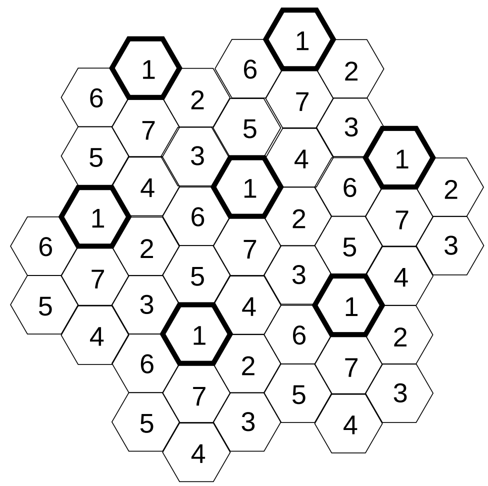

Fig. 2: Cluster structure for frequency re-use

$$D = a \cdot n \cdot R = K_1 \cdot R \tag{1}$$

II. Carrier to Interference Calculation

In this section we will derive the carrier to interference ratio C/I for a network in which no power control or adaptive modulation/coding is employed. In the last section it has been explained that the interference situation inside a considered cell is influenced by six interfering cells. If we are able to calculate the inteference due to one cell, we can easily derive the total interference situation in the considered cell. Furthermore, if we had a formula for the interference of two arbitrary cells, also un-uniform scenarios (unlike the one presented in the last section) could be easily solved. Fig. 3 illustrates two arbitrary interfering cells at a distance D.

We are interested in the C/I in a point with coordinates (x, y) in cartesian, rsp. (r, α) in polar coordinates, where the cell center is the origin of the axial system. The propagation loss is modelled according to the following formula:

$$P_R = \begin{cases} P_S \cdot (\frac{c_0}{4\pi f})^2 \cdot \frac{1}{l^\gamma} = \frac{K_2}{l^\gamma} & \text{for } l > \frac{c_0}{4\pi f} \\ P_S & \text{else} \end{cases} \tag{2}$$

where P_S is the power of the sender and P_R the received power, c_0 the speed of light, l the distance between sender and receiver and γ a propagation coefficient between 2 and 5.

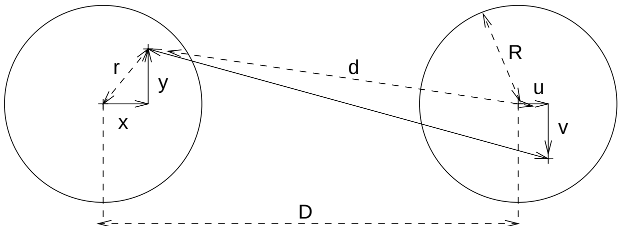

Fig. 3: Two interfering cells

Assuming the base stations being situated in the center of each cell, the received carrier level C at point (x, y) is therefore:

$$C = \begin{cases} \frac{K_2}{\sqrt{x^2+y^2}^{\gamma}} = \frac{K_2}{r^{\gamma}} & \text{for } r > \frac{c_0}{4\pi f} \\ P_S & \text{else} \end{cases} \tag{3}$$

Regarding the interference I in point (x, y) caused by the other cell, we assume that a portion p_T of the interference is caused by the terminals and a portion p_B by the base station of the interfering cell ($p_T + p_B = 1$). The interference caused by the base station is simply given by

$$I_B = \frac{K_2}{d^{\gamma}} \tag{4}$$

where d is the distance between the base station and the considered point (x, y).
To calculate the interference caused by terminals, we presume that a terminal's position is equally distributed inside a cell. We therefore average the terminal interference over the cell area of the interfering cell:

$$I_T = \frac{1}{\pi R^2} \int \int \frac{K_2}{\sqrt{(y-v)^2 + (D+u-x)^2}^{\gamma}} dudv \tag{5}$$

For $\gamma = 2$ (free-space loss) this integral can be solved by hand using polar coordinates $u = \rho \cos \phi$ and $v = \rho \sin \phi$:

$$I_T = \frac{K_2}{\pi R^2} \int_0^R \int_{-\pi}^{\pi} \frac{\rho \, d\rho \, d\phi}{(y-\rho \sin \phi)^2 + (D+\rho \cos \phi - x)^2} \tag{6}$$

By substituting $y^2 + (D-x)^2 = d^2$, $y = d \sin \beta$ and $D - x = d \cos \beta$ we get

$$I_T = \frac{K_2}{\pi R^2} \int_0^R \int_{-\pi}^{\pi} \frac{\rho \, d\rho \, d\phi}{d^2 + \rho^2 + 2\rho \cdot d \cdot \cos(\phi + \beta)} \tag{7}$$

This can be transformed to

$$I_T = \frac{K_2}{\pi R^2} \int_0^R \frac{\rho \, d\rho}{d^2 + \rho^2} \int_{-\pi}^{\pi} \frac{d\phi}{1 + A \cos \phi} \tag{8}$$

with $A = \frac{2\rho d}{d^2+\rho^2}$. After carrying out the second integration we get:

$$I_T = \frac{K_2}{R^2} \int_0^R \frac{2\rho}{d^2 - \rho^2} d\rho \tag{9}$$

This last integration leads to the final formula for the terminal interference (in the case $\gamma = 2$):

$$I_T = \frac{K_2}{R^2} \ln \left(\frac{d^2}{d^2 - R^2} \right) \tag{10}$$

We have also obtained analytical formula for $\gamma = 3$ and $\gamma = 4$, which we do not report here.

The interference by a single cell can finally be expressed as

$$I(d) = p_B \cdot I_B + p_T \cdot I_T \tag{11}$$

This interference only depends on the distance d of point (x, y) to the cell center of the interfering cell.

If we express (x, y) in polar coordinates (r, α) we obtain:

$$d = \sqrt{y^2 + (D-x)^2} = \sqrt{D^2 + r^2 - 2rD \cos(\alpha)} \tag{12}$$

The total interference in a point (x, y) is generated by all six neighbouring cells that operate on the same frequency (cf. Fig. 1). Each of the six interfering cells is rotated by $i \cdot 60$, rsp. $i \cdot \frac{\pi}{3}$ degrees ($0 \leq i \leq 5$) with respect to a reference interfering cell, where i is the index of the interfering cell. The distance of point (r, α) from each interfering cell i is given by

$$d(i) = \sqrt{D^2 + r^2 - 2rD \cos(\alpha - i \cdot \frac{\pi}{3})} \quad 0 \leq i \leq 5 \tag{13}$$

We can finally calculate the total interference and thereby the carrier to interference ratio in point (r, α):

$$\frac{C}{I}(r, \alpha) = \frac{\frac{K_2}{r^{\gamma}}}{\sum_{i=0}^{5} I(i) + N} \tag{14}$$

where $I(i)$ is calculated by inserting $d(i)$ in the formula for $I(d)$. In this formula we have also taken into account thermal noise N which is given by

$$N = F \cdot K \cdot \theta \cdot \nu \tag{15}$$

F is the noise figure of the receiver (inbetween 5 and 10), K the Boltzmann-constant ($1.38 \cdot 10^{-23}$ Ws/K), θ the temperature in Kelvin and ν the bit rate in bit/s. We will not consider N in the following.

One interesting property of eq. 14 can be illustrated for the case $\gamma = 2$ by expressing r relative to the cell radius R ($r = \eta R$ with $0 \leq \eta \leq 1$) and by considering that $D = K_1 R$:

$$\frac{C}{I}(\eta, \alpha) = \frac{1}{\tilde{I}} \tag{16}$$

with

$$\begin{aligned} \tilde{I} \quad = \quad & \sum_{i=0}^{5} \Bigg(p_B \cdot \frac{\eta^2}{K_1^2 + \eta^2 - 2\eta K_1 \cos(\alpha - i \cdot \frac{\pi}{3})} \\ & + p_T \cdot \eta^2 \cdot \ln \left(\frac{K_1^2 + \eta^2 - 2\eta K_1 \cos(\alpha - i \cdot \frac{\pi}{3})}{K_1^2 + \eta^2 - 2\eta K_1 \cos(\alpha - i \cdot \frac{\pi}{3}) - 1} \right) \Bigg) \end{aligned} \tag{17}$$

The C/I in a given point is independent of the cell radius R and just depending on the cluster-size and the relative position of the point inside its cell. This property holds true for arbitrary values of γ.

Before we derive the total system throughput from the C/I distribution in the network we will first consider how the formula have to be modified when adaptive modulation and coding are applied.

III. Influence of adaptive modulation and coding

To study the influence of adaptive modulation and coding on the system capacity we consider the case of the HIPERLAN/2 (HIgh PERformance Local Area Network) system. HIPERLAN/2 (HL/2) is a wireless LAN that has been standardised by the European Telecommunications Standardisation Institute (ETSI) in the framework of the BRAN (Broadband Radio Access Network) project and which has been completed in the years 2000 and 2001. We will not describe the details of the protocol here (the reader is referred e. g. to [3]) and instead concentrate on the adaptive modulation and coding capabilities of the system.

A. Adaptive modulation and coding in HIPERLAN/2

In HL/2 different combinations of modulation and coding schemes can be applied. All modulation schemes use *Orthogonal Frequency Division Multiplexing* (OFDM) with 52 sub-carriers. Alternative sub-carrier modulation schemes are BPSK, QPSK, 16 QAM or 64 QAM. As basic coding scheme a convolutional code with code-rate $1/2$ and constraint length 7 is used. By applying puncturing schemes alternative code rates of $3/4$ and $9/16$ can be achieved. A combination of a (sub-carrier) modulation scheme and a code rate is called a PHY-mode in the HL/2 standard. Only specific combinations of modulation and coding schemes are allowed. Table 1 gives an overview of these different PHY-modes.

Modulation	Code rate	Capacity of one OFDM-Symbol	Transm. rate
BPSK	1/2	3 byte	6 Mbps
BPSK	3/4	4.5 byte	9 Mbps
QPSK	1/2	6 byte	12 Mbps
QPSK	3/4	9 byte	18 Mbps
16-QAM	9/16	13.5 byte	27 Mbps
16-QAM	3/4	18 byte	36 Mbps
64-QAM	3/4	27 byte	54 Mbps

Table 1: HIPERLAN/2 PHY-modes

As can be depicted from Table 1 quite important gains in terms of transmission rate can be achieved with the higher PHY-modes. However, the higher the PHY-mode the more its performance is degraded by interference. This is illustrated in Fig. 4 where the *Packet Error Ratio* (PER) depending on the C/I is shown for the different PHY-modes. The curves have been derived by link level simulations.

To get realistic throughput values we first consider the

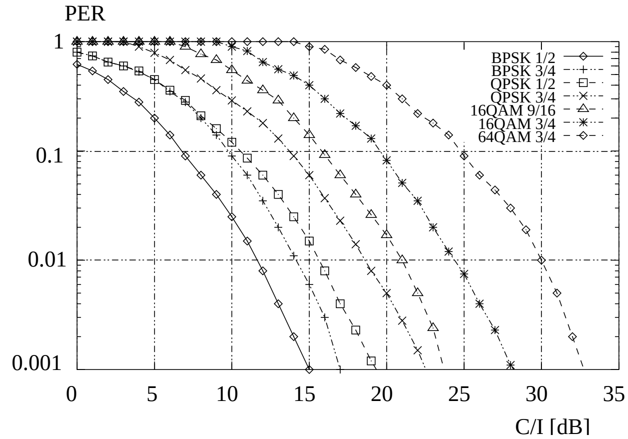

Fig. 4: PER versus C/I

throughput of the Medium Access Control (MAC) protocol of HL/2 T_{MAC}. In [4] it has been shown that this throughput is given by

$$T_{MAC} = \left\lfloor \frac{L_{LCH}}{\left\lceil \frac{54}{BpS_{LCH}} \right\rceil} \right\rfloor \cdot \frac{48 \cdot 8}{2\,\text{ms}}. \tag{18}$$

In this equation L_{LCH} is the number of so-called *Long Channels* (LCH) in the MAC-frame which will be considered as a given number in the following. BpS_{LCH} is the number of bytes that are transmitted by one OFDM-symbol (depending on the PHY-mode). The BpS_{LCH} values can be found in the third column of Table 1.

To obtain the final throughput the *Automatic Repeat Request* (ARQ) mechanism of HL/2 has to be taken into account. The ARQ protocol of HL/2 is very similar to a so-called *Selective Repeat Reject* mechanism. It is known that this scheme results in the throughput (cf. [3]):

$$T_{DLC} = T_{MAC} \cdot (1 - PER) \tag{19}$$

Inserting eq. 18 and the PER versus C/I relations of Fig. 4 into eq. 19 we obtain the final throughput versus C/I relations for the different PHY-modes illustrated in Fig. 5.

From Fig. 5 it can be depicted that to maximise the throughput only five PHY-modes should be applied. The C/I values, at which a PHY-mode switch should occur, are marked in Fig. 5. We finally obtain the following intervalls:

$$\begin{array}{lllll} 20.1 & < & C/I & & : \; 64QAM3/4 \\ 15.6 & < & C/I & \leq 20.1 & : \; 16QAM9/16 \\ 10.3 & < & C/I & \leq 15.6 & : \; 16QAM3/4 \\ 7.8 & < & C/I & \leq 10.3 & : \; QPSK3/4 \\ & & C/I & \leq 7.8 & : \; QPSK1/2 \end{array} \tag{20}$$

In this determination of C/I intervalls we have assumed that a throughput maximisation is aimed at. Delay optimisation is not considered.

B. Network throughput calculation

We now come back to our analysis of the system throughput. As it has been derived in the previous section, the PHY-mode,

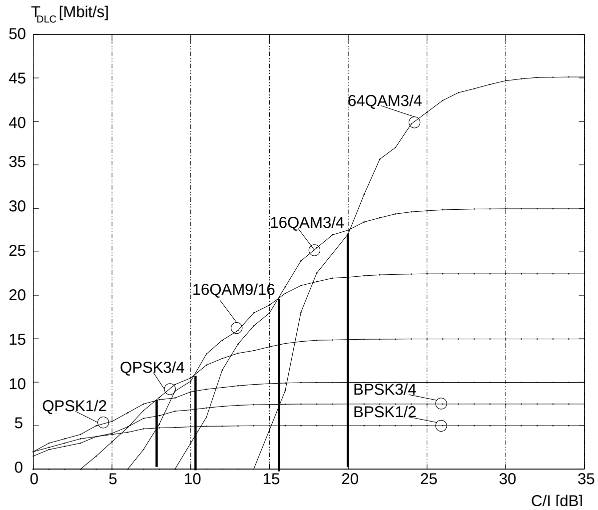

Fig. 5: Throughput versus C/I

that a terminal can apply, and thereby the achievable data rate, depends on the C/I ratio. Inside a radio cell the C/I decreases from the center to the border of the cell, which can be deduced from equation 14 and which is also intuitively obvious. Furthermore, numerical evaluations of eq. 14 have shown that the C/I distribution inside a cell is (almost) independent of the angular coordinate α. Therefore, inside a cell regions in the form of centric rings will result, in which a certain combination of modulation and coding scheme can be applied (cf. Fig. 6).

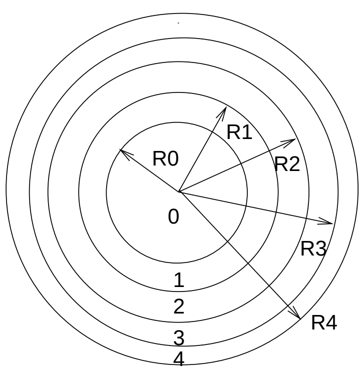

Fig. 6: Regions of PHY-mode employment

For the calculation of the interference we approximate the borders of the different zones by circles, the radii of which correspond to the C/I values at which a terminal or base station switches from one PHY-mode to the next (cf. eq. 20).

Taking into account the application of adaptive modulation and coding, the formula derived in section II have to be modified. It has now to be considered that for the transmission of the same amount of data, transmission with a lower PHY-mode lasts much longer than transmission with a higher PHY-mode resulting in a higher interference contribution to the neighbouring cells.

If we assume that the amount of data to be transmitted is equally distributed over the whole network, the relative duration of transmission activity at a given point is inversely proportional to the throughput that can be achieved at this position. We have therefore taken the reciprocal values of the maximum throughput curves in Fig. 5 to obtain a relation of the transmission duration versus the C/I. This can be transformed into a spatial distribution of the transmission duration inside a cell. After dividing this distribution of the transmission duration by its integral, a function for the relative transmission duration depending on the relative position inside a cell (r/R) is derived (cf. Fig. 7).

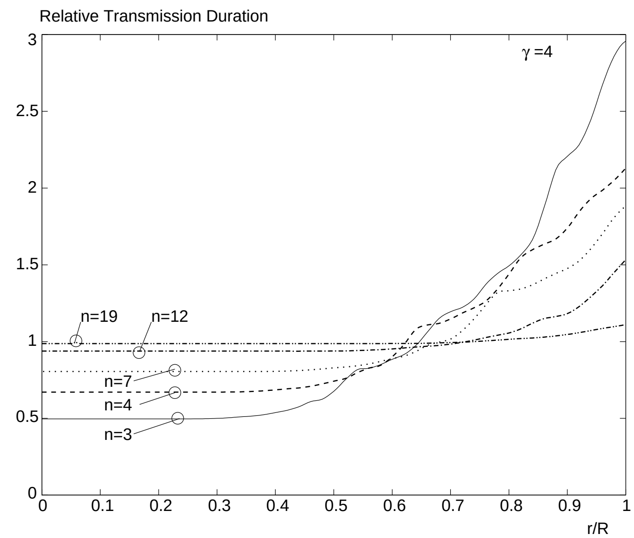

Fig. 7: Relative Transmission Duration depending on the position

To calculate the final C/I distribution in the network, we make an iterative approach. We first assume a constant transmission duration in the six interfering cells, i. e. not considering the adaptive modulation/coding. According to eq. 14 we will then obtain a C/I distribution inside a cell. With this C/I distribution we derive the spatial distribution of the relative transmission duration in the cell (Fig. 7). In a next iteration we presume this distribution of relative transmission duration in the six interfering cells, i. e. we now model the adaptive modulation/coding to calculate the interference in a considered cell. Thereby we obtain an improved C/I distribution inside the cell. This distribution can in a further iteration be used to improve the interference calculation, etc. Our numerical evaluations have shown that already after the first iteration an almost exact C/I distribution is obtained and that further iterations lead to very minor changes.

Considering the relations illustrated in Fig. 5 we have at the same time obtained the throughput distribution inside the cell. In a last step we integrate this throughput distribution over the entire cell and divide it by the area of the cell to obtain the average system throughput. In this case we assume again an hexagonal form of the cells in order not to count twice the overlapping zones of the circular cells:

$$T_{av} = \frac{6}{3/2\sqrt{3}\, R^2} \int_{-\frac{\pi}{6}}^{\frac{\pi}{6}} \left(\int_0^{\frac{\sqrt{3}}{2}\frac{R}{\cos\alpha}} T_{DLC}(r,\alpha)\, r\, dr \right) d\alpha \tag{21}$$

We have carried out the described iterative approach numerically for different cluster sizes n and propagation factors γ. In the numeric calculation we have assumed a constant transmitter power of 0.5 W because in HL/2, due to regulatory requirements, the average transmission power has to be 3 dB below the maximum power of 1 W (in the outdoor-band). Regarding the relation between re-use distance D and cell radius R the scalar factors in Table 2 apply (cf. eq. 1).

Cluster-size n	Factor K_1
3	3
4	$\sqrt{3}+2=3.732$
7	$\sqrt{21}=4.583$
12	6
19	$\sqrt{57}=7.550$

Table 2: Factors between D and R for different cluster-sizes

The results of our analysis are displayed in Fig. 8 for $\gamma=2$ and $\gamma=4$.

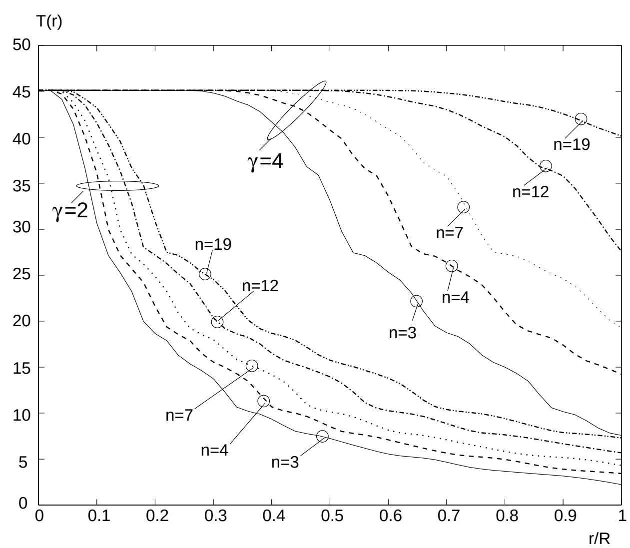

Fig. 8: Achievable throughput at radius r inside a cell

In the final version of this paper we will also include numerical results for the average system throughput depending on the cell radius R (according to eq. 21).

Another interesting result of our numerical calculations has been that the application of adaptive modulation/coding had an (almost) neglectable effect on the interference situation in the cells compared to the initial situation without adaptation of PHY-modes (see also the analysis in the following section). However, there is a significant increase in throughput at a given C/I because always the optimum PHY-mode is employed.

IV. Influence of power control

We assume that with optimum power control the terminals exactly compensate an increase in path loss as far as the maximum transmission power (of 1 W in HL/2) is not reached. To gain a better understanding of the influence of power control on the interference situation we have calculated the average terminal interference I_T like in eq. 6 but now considering that the transmission power is increased with the distance of the terminal from the base station (according to ρ^m):

$$I_T = \frac{K_2(m+2)}{2\pi R^{(m+2)}} \int_0^R d\rho \left(\int_{-\pi}^{\pi} \frac{\rho\, \rho^m d\phi}{\sqrt{(y-\rho\sin\phi)^2 + (D+\rho\cos\phi - x)^2}^{\gamma}} \right) \tag{22}$$

We have assumed that the average power of all terminals is upper bounded as it is the case for HL/2 where the average power has to be smaller than 0.5 W. This is accounted for by the normation factor $\frac{2}{m+2}R^m$.

We have tested the influence of power control with m varying from 1 to 15 and found that the power control has in most cases a neglectable influence on the interference in the neighbouring cells. This also explains why adaptive modulation/coding had a neglectable influence on the interference.

In Table 3 the relative error that we make when approximating the interference by the no-power-control-formula is given as approximation 1.

γ	m	Cluster size n	Rel. Error approx. 1 [%]	Rel. Error approx. 2 [%]
2	2	3	1.1399	5.2002
2	2	4	0.6820	3.1709
2	2	7	0.4331	2.0342
2	2	12	0.2439	1.1549
4	4	3	7.7316	22.5543
4	4	4	4.4244	13.4953
4	4	7	2.7552	8.5692
4	4	12	1.5340	4.8266

Table 3: Influence of power control on the interference

In formula 14 for the C/I the transmission power can normally be cancelled down. However, with power control we have to take into account that the terminals in the interfering cells transmit on average with P_{av} (equal to 0.5 W in the case of HL/2), whereas for a specific terminal in the considered cell a transmission power up to P_{max} (equal to 1 W in the case of HL/2) could be used.

The power control can be based on different link quality criteria like *Received Signal Strength* (RSS), PER or C/I. We assume C/I based power control in the following. With perfect power control, a desired constant C/I inside a ring region can be maintained until P_{max} is reached. If P_{max} is reached the C/I starts to drop for increasing r until a C/I threshold, at which a PHY-mode switch is carried out.

We approximate the interference by eq. 23 in the following.

$$I = 6\frac{K_2}{D^\gamma} \tag{23}$$

where D, as above, is the frequency re-use distance. The error we make with this approach is also shown in Table 3 in the last column as approximation 2.

With this last approximation we obtain the following formula for the radii R_j at which a PHY-mode switch is carried out:

$$\begin{aligned} R_0 &= \left(\frac{P_{max}}{6 \cdot 20 \cdot P_{av}}\right)^{\frac{1}{\gamma}} D = \frac{1}{240^{\frac{1}{\gamma}}} K_1 \cdot R && (24) \\ R_1 &= \left(\frac{P_{max}}{6 \cdot 16 \cdot P_{av}}\right)^{\frac{1}{\gamma}} D = \frac{1}{192^{\frac{1}{\gamma}}} K_1 \cdot R && (25) \\ R_2 &= \left(\frac{P_{max}}{6 \cdot 10 \cdot P_{av}}\right)^{\frac{1}{\gamma}} D = \frac{1}{120^{\frac{1}{\gamma}}} K_1 \cdot R && (26) \\ R_3 &= \left(\frac{P_{max}}{6 \cdot 7 \cdot P_{av}}\right)^{\frac{1}{\gamma}} D = \frac{1}{84^{\frac{1}{\gamma}}} K_1 \cdot R && (27) \end{aligned}$$

For a given cluster-size n, respectively factor K_1, only PHY-modes up to k might be actually used. k is the smallest $j \in \{0, 1, 2, 3, 4\}$ for which $R_j \geq R$. This R_k is then set to R.

We finally have to derive the target C/I which is maintained until P_{max} is reached. Unfortunately, the target C/I can not be chosen by the system designer, if we assume that a transmission power of P_{av} has to be used by all terminals on average. This condition can be formulated for each ring in the form:

$$\frac{1}{\pi(R_j^2 - R_{j-1}^2)} \left(2\pi \int_{R_{j-1}}^{\tilde{R}_j} P_{max} \frac{\rho^\gamma}{\tilde{R}_j^\gamma} d\rho + \pi(R_j^2 - \tilde{R}_j^2) P_{max}\right) = P_{av} \tag{28}$$

We have designated with $\tilde{R}_j$ the radius at which P_{max} is reached in the ring j.

Eq. 28 can be simplified as follows

$$\frac{1}{(R_j^2 - R_{j-1}^2)} \left(\frac{2}{\gamma+1}\left(\tilde{R}_j - \frac{R_{j-1}^{\gamma+1}}{\tilde{R}_j^\gamma}\right) + (R_j^2 - \tilde{R}_j^2)\right) = \frac{P_{av}}{P_{max}} \tag{29}$$

After having calculated all R_j according to eq. 24, 25, 26, 27 (R_4 is equal to R, if $k = 4$), $\tilde{R}_j$ can be calculated with eq. 29 for $j = 0, \ldots, k$.

The target C/I for ring j, which corresponds to a constant throughput value T_j, is given by

$$C/I_j = \frac{1}{6} \frac{P_{max}}{P_{av}} \left(\frac{D}{\tilde{R}_j}\right)^\gamma \tag{30}$$

We are now able to determine the average system throughput in the case of power control. It can be calculated according to eq. 31.

$$T_{av} = \sum_{j=0}^{k} T_{av}(j) \tag{31}$$

with

$$T_{av}(j) = \frac{1}{(R_j^2 - R_{j-1}^2)} \left((\tilde{R}_j^2 - R_{j-1}^2) \cdot T_j + \int_{\tilde{R}_j}^{R_j} T_{DLC}\left(\frac{1}{6}\frac{P_{max}}{P_{av}}\left(\frac{D}{r}\right)^\gamma\right) r\, dr\right) \quad \text{for } j < k \tag{32}$$

and

$$T_{av}(k) = \begin{cases} \frac{1}{3\left(\sqrt{3}/2\ R^2 - R_{k-1}^2\right)} \Big\{(\tilde{R}_k^2 - R_{k-1}^2) \cdot T_k \\ + \int_{-\frac{\pi}{6}}^{\frac{\pi}{6}} \int_{\tilde{R}_k}^{\frac{\sqrt{3}}{2}\frac{R}{\cos\alpha}} T_{DLC}\left(\frac{1}{6}\frac{P_{max}}{P_{av}}\left(\frac{D}{r}\right)^\gamma\right) rdrd\alpha\Big\} \\ \text{if} \quad \tilde{R}_k \leq \frac{\sqrt{3}}{2} R \\ \frac{1}{3\left(\sqrt{3}/2\ R^2 - R_{k-1}^2\right)} \Big\{T_k \cdot \int_{-\frac{\pi}{6}}^{\frac{\pi}{6}} d\alpha\, (\\ \int_{R_{k-1}}^{\min\{\tilde{R}_k, \frac{\sqrt{3}}{2}\frac{R}{\cos\alpha}\}} rdr) \\ + 2\int_{\cos\left(\frac{\sqrt{3}/2R}{\tilde{R}_k}\right)}^{\frac{\pi}{6}} d\alpha\, (\\ \int_{\tilde{R}_k}^{\frac{\sqrt{3}}{2}\frac{R}{\cos\alpha}} T_{DLC}\left(\frac{1}{6}\frac{P_{max}}{P_{av}}\left(\frac{D}{r}\right)^\gamma\right) rdr)\Big\} \\ \text{if} \quad \frac{\sqrt{3}}{2} R < \tilde{R}_k \leq R \end{cases} \tag{33}$$

Numerical results for the average system throughput in the power control case will be included in the final version of this paper.

V. Conclusions

In this work the system throughput has been calculated for the modulation/coding types as well as the Physical and MAC Layer characteristics of the HIPERLAN/2 system. Nevertheless the presented approach can be applied under the assumption of different propagation laws and system characteristics. In any case the presented analysis represents a valuable tool to evaluate the system performance resulting from different design choices in network planning and/or terminal/base-station algorithms.

VI. References

[1] W. C. Y. Lee, "New Cellular Schemes for Spectral Efficiency," *IEEE Trans. On Vehic. Techn.*, vol. 36, pp. 188 – 192, Nov. 1987.

[2] W. C. Y. Lee, "Spectrum Efficiency in Cellular," *IEEE Trans. On Vehic. Techn.*, vol. 38, pp. 69 – 75, May 1989.

[3] B. Walke, *Mobile Radio Networks*. Chichester, Sussex, UK: Wiley & Sons Ltd., 1999.

[4] B. Walke, N. Esseling, J. Habetha, A. Hettich, A. Kadelka, S. Mangold, and J. Peetz, "IP over Wireless Mobile ATM – Guaranteed Wireless QoS by HiperLAN/2," *Proc. of the IEEE*, vol. 89, Jan. 2001.